



Power Electronic Systems
Laboratory

© 2014 EPE

EPE Journal, Vol. 23, No. 3, pp. 36-47, September 2014

Mission Profile Based Optimization of a Wearable Power System

I. Kovacevic,
J. W. Kolar,
S. D. Round,
M. Vasic,

This material is published in order to provide access to research results of the Power Electronic Systems Laboratory / D-ITET / ETH Zurich. Internal or personal use of this material is permitted. However, permission to reprint/republish this material for advertising or promotional purposes or for creating new collective works for resale or redistribution must be obtained from the copyright holder. By choosing to view this document, you agree to all provisions of the copyright laws protecting it.



Eidgenössische Technische Hochschule Zürich
Swiss Federal Institute of Technology Zurich

Mission Profile Based Optimization of a Wearable Power System

Ivana F. Kovačević, Johann W. Kolar, Power Electronic Systems Laboratory, ETH Zurich, Switzerland
 Simon D. Round, ABB Switzerland, Turgi, Aargau, Switzerland
 Miroslav Vasić, Universidad Politecnica de Madrid, Centro de Electronica Industrial, Spain

Keywords: Buck converter, Hybrid power system, Mission profile, System optimization, Wearable power system

Abstract

A Wearable Power System (WPS) is a portable power source utilized primarily to power the modern soldier's electronic equipment. Such a system has to satisfy output power demands in the range of 20 W...200 W, specified as a 4-day mission profile and has a weight limit of 4 kg. To meet these demands, an optimization of a WPS, comprising an internal combustion (IC) engine, permanent magnetic three-phase electrical motor/generator, inverter, Li-batteries, DC-DC converters, and controller, is performed in this paper. The mechanical energy extracted from the fuel by IC engine is transferred to the generator that is used to recharge the battery and provide the power to the electrical output load. The main objectives are to select the engine, fuel and battery type, to match the weight of fuel and the number of battery cells, to find the optimal working point of engine and to minimize the system weight. To provide the second output voltage level of 14 V_{DC}, a separate DC-DC converter is connected between the battery and the load, and optimized for the specified mission profile. A prototype of the WPS based on the optimization presented in the paper results in a total system weight of 3.9 kg and fulfils the mission profile.

Introduction

In 2007, the USA Department of Defence (DOD) announced the Wearable Power Competition with intent to encourage teams and individuals to build a wearable power system with the capability to supply an average of 20 W for 4 days, i.e. 1920 Wh, with peak power up to 200 W, and have a total system weight of less than 4 kg [1]. According to the specifications, the minimal required average gravimetric energy density of system is 480 Wh/kg (1920 Wh/4 kg = 480 Wh/kg). Two output voltages are required: 28 V_{DC} (range of 20-32 V_{DC}) and 14 V_{DC} (range of 10-16 V_{DC}). The primary purpose of such a power supply is to be an integral part of an infantry soldier's equipment but also it could be used in other commercial applications such as a power source for emergency rescue services.

The main challenge of building the wearable power system is that it should be optimized for the given mission (load) profile and at the same time it should fulfil weight constraints. The mission profile defined by the competition rules comprises three types of load, Base Load, Communications Load and Video Feed Load that sequentially repeat during the operating time. Four power levels of 3 W, 20 W, 50 W and 200 W within these load periods are specified [2] (see Table I).

To meet the competition objective a small scale combustion engine is chosen and the system structure as presented in Fig. 1 is selected [3]. The majority of the required energy is stored in a liquid gasoline fuel. The energy is extracted from the fuel as mechanical energy by a small-scale, single-cylinder internal combustion (IC) engine. The theoretical aspects of these engines used for portable power generation are covered in [4]. This engine in turn rotates a permanent magnetic, three-phase electrical generator. A power electronics converter, together with the engine controller, regulates the flow of the generator's output power. A rechargeable battery is used as limited, intermediate energy storage. The power provided from the generator is used to recharge the battery and/or provide the power to the electrical output loads. The electrical output loads are supplied either directly from the battery or through a DC-DC converter.

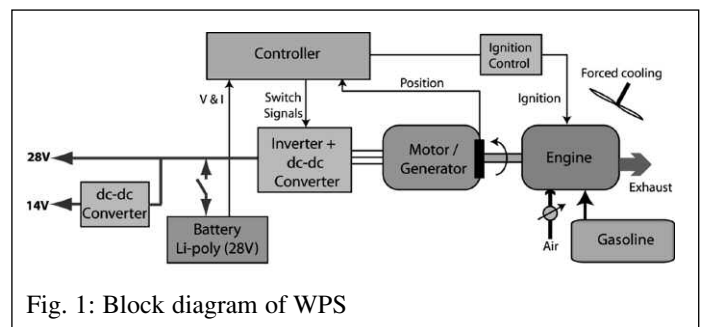


Fig. 1: Block diagram of WPS

The system in Fig. 1 is a hybrid system that has been investigated extensively in last years for various industrial applications e.g. grid power supplies [5], cable cars [6], aircraft [7], cars [8, 9], railway [10, 11], military [12-14] with the intent to increase system efficiency and to have a better energy supply balance when combining two or more energy sources. Depending on the applications, different combinations of primary and secondary energy sources have been exploited: fuel cells/rechargeable batteries, fuel generators/rechargeable batteries, and photovoltaic/wind/diesel generators. For optimizing a system comprising two or more energy storages a cost function that includes the parameters of interest like weight, size, emission, and energy consumption has to be defined. The cost function is then minimized using an optimization algorithm [15-18].

The main objective of the overall system design is to select engine type and size, fuel and battery type and to match the weight of fuel and the number of battery cells in order to satisfy all input conditions and to find the optimal working point of engine when it is operated and the minimal overall weight. Considering different output voltage levels, the output DC-DC converters have to be added to the system and hence optimized to keep total system weight less than 4 kg and to achieve the highest converter efficiency under the variable mission profile.

Next section of the paper presents the requirements defined by the competition rules, the wearable power system description and the

definition of the optimization problem, followed by the structural modeling of the system together with the set of system equations. Next, the approach to overall system optimization and the results are discussed. Finally, the main topic is the power electronics system output stage i.e. the additional DC-DC converter. The DC-DC converter optimization under the given mission profile is investigated and the experimental performance of the designed converters is shown. The conclusion summarizes the final system design parameters obtained by the optimization procedures from Matlab and the performance of the designed DC-DC buck converter prototype.

Wearable Power System

The requirements of the wearable power system, the chosen system components and two-mode system operation are presented in this section. After analyzing several different possibilities for energy storage/generation used in combination or solely, an internal combustion engine and rechargeable batteries are selected.

Requirements

Minimum power delivery requirements for the system are [1]: (1) time duration of 4 days (96 h), (2) average power of 20 W, (3) peak power of 200 W, (4) voltage output $14 V_{dc}$ (range of 10-16 V) or $28 V_{dc}$ (range of 20-32 V).

Each wearable power system is tested against a specific load profile during the bench test. Three types of load repeat throughout the test: Base Load, Communications Load and Video Feed Load comprising four voltage levels of 3 W, 20 W, 50 W and 200 W, cf. Fig. 2. The details describing a 24-hour load profile are summarized in Table 1 [2].

The 3 W load level is applied for the longest time (78 %), while the 200 W load is applied 7 % of the time. Considering the amount of energy, 200 W load uses 67 % of the total energy while the other three loads consume approximately 11 % each. The Video

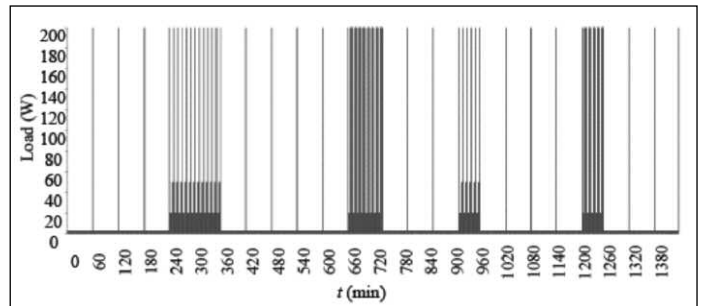


Fig. 2: 24 hour mission profile: Base Load – 4 cycles, Communication Load – 12 cycles, Base Load – 5 cycles, Video Load – 8 cycles, Base Load – 3 cycles, Communication Load – 5 cycles, Base Load – 5 cycles, Video Load – 5 cycles, Base Load – 3 cycles.

Feed Load is the most critical part as the system must support 20 W-200 W power periods taking place every 5 minutes for up to 1 hour. This results in an average video load power of 110 W, which is much higher than the 96 hours average of 20 W. Such a mission profile, cf. Fig. 2, presents the main difficulty since the peak load is ten times higher than the average load. The power pack has to be designed to provide 0-200 W from the 14 V and/or 28 V outputs.

Since the WPS has to satisfy the load and weight demands, the system design is not straight forward and an optimisation procedure is conducted in order to build a system with the highest efficiency, optimal weight and all of the desired capabilities.

System design/energy storage

Three different possibilities for energy generation/storage are analyzed:

- non-rechargeable (primary) batteries solely;
- hydrogen/methanol fuel cells and rechargeable (secondary) batteries;
- internal Combustion (IC) engine and rechargeable batteries.

Table 1: 24 hours load profile example					
Load Type	Load [W]	Time [min]	Cycles	Energy [Wmin]	Avg. [W]
Base Load	3	59	4	708.0	6.3
	200	1		800.0	
Communication	20	6	12	1440.0	47.0
	50	3		1800.0	
	200	1		2400.0	
Base Load	3	59	5	885.0	6.3
	200	1		1000.0	
Video Feed Load	20	5	8	800.0	110.0
	200	5		8000.0	
Base Load	3	59	3	531.0	6.3
	200	1		600.0	
Communication	20	6	5	600.0	47.0
	50	3		750.0	
	200	1		1000.0	
Base Load	3	59	4	708.0	6.3
	200	1		800.0	
Video Feed Load	20	5	5	500.0	110.0
	200	5		5000.0	
Base Load	3	59	3	531.0	6.3
	200	1		600.0	

Non-rechargeable (primary) batteries are not the best choice for a soldier wearable system as they have to be quite heavy in order to provide power for a time period of few days. Even though non-rechargeable batteries with high energy density of up to 590 Wh/kg can be found on the market [19], their applicability to the wearable system is not feasible as they can deliver only limited currents. Due to discharge current restrictions, the idea of a single primary battery pack supplying the load for the whole specification time is not considered.

As the second possible solution for energy storage hydrogen fuel cells are analyzed. Fuel cells have high specific energy, high efficiency and improved environmental performance and they can be incorporated into rechargeable energy storage systems [20]. However, besides all these advantages, hydrogen must be under high pressure and requires storage tanks with special construction which makes them heavy, so they are not a promising candidate to meet construction requirements. In the case at hand the minimum weight of hydrogen H-tank would be 2-3 kg i.e. more than a half of the allowed system weight. The further analysis leads to liquid fuels e.g. methanol and gasoline. As the technology of the small, low power methanol fuel cells has advanced, a methanol fuel cell seems feasible for the WPS design but requires a custom solution rather than an off-the-shelf solution. Accordingly, due to the limited time frame and other construction requirements a solution based on a small Internal Combustion (IC) Engine was preferred. For the combination of an IC Engine and a rechargeable (secondary) battery pack the assumption that the chosen fuel mixture has sufficient stored energy is investigated through the following calculation. By assuming an efficiency of a small capacity engine of 10 % (much lower than 20 % typical for automotive engine), the energy density of gasoline is 43 MJ/kg, and a 10-hour engine run-time is required to produce the 2000 Wh if the engine-generator output is 200 W (6.91 MJ for the competition) a total required fuel weight of 1.6 kg can be calculated. This is less than half the maximum weight of 4 kg and therefore it seems possible that an engine based system can compete, even taking into account the additional weight of the engine, generator and battery. The small-scale engines are typically designed to operate using methanol as fuel, however methanol has a lower energy density of 20 MJ/kg and therefore the system would require approximately 3.4 kg of fuel, which is not feasible unless the engine efficiency is increased substantially.

Consequently, the designed wearable power system presented in Fig. 1 consists of batteries and a fuel tank for energy storage, the engine for extracting the energy from the fuel by combustion and converting it to mechanical rotation, the three phase generator with inverter output for mechanical to DC electrical power conversion, power electronics converters for adjusting the voltage levels and the controller for monitoring and regulating all changes inside the system.

Combustion engine

The engine is a standard model-aircraft four-stroke single-cylinder engine from O.S. Engines, Japan [21]. The fuel consumption should be as low as possible so that a reasonable fuel weight can satisfy the four days load profile and the used fuel has to have high heating value. The standard small engines are designed for methanol operation but gasoline can be also burned if a gasoline carburettor and additional ignition system and spark plug are implemented. Therefore, two fuel mixtures are considered: the methanol/oil, and the gasoline/oil. The calculation is performed with the assumption of 20 MJ/kg for the heating value of the methanol mixture and 43 MJ/kg for the gasoline/oil mixture. The real heating value depends on the amount of oil burned in combustion process e.g. in the case of the methanol mixture, it lies somewhere between 17 MJ/kg and 22.6 MJ/kg. Forced cooling is provided for both engine and motor/generator by a 10 W electric fan.

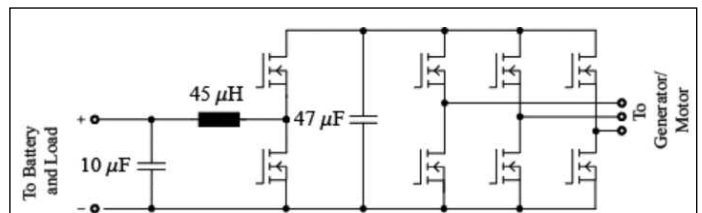


Fig. 3: Interface power electronics between battery and generator/motor

Table 2: Battery types used in optimization procedure

Battery	Type 1	Type 2	Type 3	Type 4
Manufacturer	A123System	VARTA	VARTA	KOKAM
Battery Type	Li-Ion	Li-Poly.	Li-Poly.	Li-Poly.
Nominal Capacity [Ah]	2.3	0.92	0.126	4.8
Nominal Voltage [V]	3.3	3.7	3.7	3.7
Charge Current [A]	3	0.92	1.126	4.8
Max. Discharge Current [A]	70	1.84	2.252	96
Weight [g]	70	17	24	115
Gravimetric Energy [Wh/kg]	110	170-200	114	

Motor/generator

The motor/generator is a 220 W three-phase permanent magnet brushless DC motor based on a commercially available stator winding from ATE GmbH [22] and a custom rotor that directly attaches to the engine shaft. Therefore no additional bearings are required for the generator since the engine bearings are used, thus the total system weight is reduced. The output voltage from generator is proportional to rotating speed of rotor shaft. When it operates as a generator, the peak output voltage is 31 V at 10,000 rpm rising to 38 V at 12,000 rpm. This allows the engine to operate over a wide speed range and ensures that the generator voltage output is greater than the maximum battery voltage. To start the engine, the generator is used as motor. A speed of up to 4000 rpm is required to start the engine with the battery being used as the energy source. The motor AC phase voltages and currents are generated by the power electronics AC-DC converter operating as inverter (DC-AC operation).

AC/DC converter

The main function of the power electronics converter (six-switch MOSFET inverter/rectifier) is to act as a rectifier (AC-DC operation) to convert the three phase AC voltage generated by the generator into a DC voltage for charging the battery. Since the engine speed is variable and therefore the generator output voltage is variable, a simple synchronous buck converter is placed between DC output of converter and the battery pack, as shown in Fig. 3. With this DC-DC converter the charging current of the battery and the loading of the engine can be controlled. The high efficiency is achieved by using low on-resistance, low voltage MOSFETs.

Battery pack

Today one of the most promising rechargeable energy storage systems are Li-Ion based batteries, which experienced continuous improvement over the last years. Therefore, advanced rechargeable Li-Ion based batteries are selected as the intermediate energy storage. The properties of interest for battery selection are gravi-

metric energy density, capacity, operating voltage, operating temperature, service life, weight per battery cell, and maximal charge/discharge current. Four battery types with relevant characteristics summarized in Table 2 [23-26] are considered.

DC-DC converter

To provide either 14 V_{DC} or 28 V_{DC} output a separate DC-DC converter is connected between the battery and the load output. It is a custom designed converter independently controlled and additionally optimized.

Control electronics

The control electronics is used for two main tasks. Firstly, for the monitoring of the battery pack's state of charge (SOC), and secondly for starting and controlling the engine and electric power generation, which is used to charge the battery pack. The power for the control electronics is supplied from the Li-Ion/Li-Polymer batteries. The control algorithms are implemented in a TI 2808 DSP.

Operation modes

The way the system functions can be simply described in the following two states manner.

Mode 1: Engine turned off

When the engine is turned off and the power output is supplied only by batteries; the batteries provide energy to the output as long as their state of charge (SOC) is above 20 % to ensure that the engine can be started; SOC is defined as the percentage of the maximum possible charge stored in the battery [27]. SOC is determined by measuring the battery current. Under light load operation the open-circuit voltage can be used as a secondary method to determine the battery SOC.

Mode 2: Engine turned on

When the engine is turned on the batteries are charged and the power is delivered to the output. The engine is stopped when the batteries are charged to 80 % SOC [28] as it is not possible to achieve full charging, since this would require the engine to be run at reduced speeds, low power and correspondingly low efficiency.

System modeling

The starting point of the optimization procedure is the physical modeling of the overall system. The WPS is structurally divided into functional blocks and its electrical behaviour is described by a set of mathematical equations. Engine and generator measurements have been conducted to determine the mechanical/electric power, the fuel flow and the engine and generator efficiency as functions of engine speed. The measured data were interpolated to derive the functions that define the corresponding dependences.

System equation

Equations (1) - (8) are used to mathematically describe the system. To simplify the system in the first step, the engine, generator, inverter and converter were only characterized by their power efficiencies. Equations (1) - (3) concern the power equilibriums of the system.

$$W_{\text{fuel}} = LHW \cdot m_f \quad (1)$$

$$P_{\text{el1}} = W_{\text{fuel}} \cdot \eta_{\text{eg}} \quad (2)$$

$$P_{\text{el2}} = P_{\text{el1}} \cdot \eta_C \quad (3)$$

where LHW is the low heating value of the used fuel in J/kg, m_f is the fuel flow in g/min, W_{fuel} is the power produced by fuel burning, η_{eg} is the efficiency of generator and engine together, P_{el1} is the electrical power at the output of generator, η_C is the efficiency of AC-DC converter and P_{el2} is the electrical power at the output of AC-DC converter or at the input of battery units and load, cf. Fig. 3.

The battery is modeled as a voltage source with the nominal voltage value E_b and an internal resistance R_b . The battery's charging $I_{b,\text{chg}}$ is described by (4) coming from the power equilibrium at the battery input/output ports. Hence $P_{b,\text{in}}$ is the power for charging the battery while $P_{b,\text{out}}$ is the power that the battery provides.

$$I_{b,\text{chg}} = \frac{1}{2} \frac{E_b}{R_b} + \frac{1}{2} \sqrt{\left(\frac{E_b}{R_b}\right)^2 + 4 \frac{P_{b,\text{in}}}{R_b}} \quad (4)$$

Equation (4) is used for calculating the battery state of charge, SOC (5) [29],

$$SOC = \eta_{\text{chg}} / (60 \cdot C_{\text{cap}}) \int_0^{t_c} I_{b,\text{chg}} dt \quad (5)$$

where C_{cap} is the battery capacity in Ah, η_{chg} is the efficiency of the charging operation, and t is time expressed in minutes. When the engine is turned off, the battery solely provides power to the output. The power equilibriums for engine turn off and on states are described respectively by (6) and (7),

$$P_{\text{out}} = P_{b,\text{out}} \quad (6)$$

$$P_{\text{el2}} = P_{\text{out}} + P_{b,\text{in}} \quad (7)$$

The number of batteries in series, n , is calculated by (8), with the output voltage V_{out} of either 14 V_{dc} or 28 V_{dc} ,

$$n = [V_{\text{out}}/E_b] \quad (8)$$

For solving the system model, all previously defined parameters must be known. The battery data sheets provide the information about the different battery types, while measurements are conducted to determine the engine/generator characteristics: the dependencies of the mass fuel flow, the efficiency and the output power on the different engine/generator speeds. In the following subsection, the engine and generator modelling using the measured and calculated dependencies is described.

Engine/generator modeling

There are a number of parameters affecting the total efficiency of the engine plus generator, such as the air-fuel ratio and construction of the generators. In this investigation, the parameters were limited since a fixed carburettor was used and no throttling of the engine was possible. Therefore, the main factor was to determine operating point, engine speed that gave the maximum efficiency.

The set-up for measuring the characteristics of engine and generator consists of the OS FS-30 Surpass IC (volume 0.30 in³, i.e. 4.9 cm³) engine [21] and a permanent magnet three-phase brushless motor/generator. The motor is coupled to the engine to act as load. The tests involved measuring the output electrical power and fuel mass flow as a function of engine speed (rpm) for a number of discrete operating points. Two tests have been conducted, one using the gasoline/oil and the other using the methanol/oil mixture, as a fuel.

According to the measured values of the electrical power at the output of generator, the fuel mass flow and the engine speed, the corresponding dependencies (the output power of generator, the

engine/generator efficiency and the fuel mass flow vs. speed) shown in Fig. 4 - Fig. 6 are derived using polynomial fitting methods. Depending on the heating values of the used fuel, the efficiency of generator and engine system is not directly measured but derived from the measured output power and mass flow values at the different speeds. Fig. 4-6 show the measured data points and curve fits for use in a system optimization program. This particular engine has an electrical output power of 200 W at 12,000 rpm and a fuel mass flow of less than 2.5 g/minute.

As the highest speed of approximately 14000 rpm is not possible to achieve with the OS FS-30 Surpass working on gasoline, the final fitting function for the output power dependency on speed is modified so that it does not follow the polynomial function above the maximal power any more but stays constant. The maximal efficiency is 12.9 % and it is achieved at 11599 rpm.

System optimization problem

To provide enough electrical power for the critical output load situations and satisfy the weight constraints, the engine should be small and have relatively high efficiency. On the other hand to fulfil voltage levels solely by batteries and to handle the charging current delivered by motor and engine at the battery input, a battery pack consisting of *m* parallel strings and *n* batteries in series per string is needed. Namely charging current is limited by the number of batteries in parallel while the output voltage determines the number of batteries in series.

Optimization of the wearable power system can be seen as making the compromise between the number of batteries in the battery storage system, the total volume of fuel and the type of engine. In general, having more fuel, a smaller engine (with lower efficiency generating lower charging current) can be used implying less battery cells in parallel, and vice versa having more cells in parallel a heavier engine can be implemented (with higher efficiency) and less fuel would be necessary. The crucial part of optimization problem lies in optimizing the battery storage to meet power-speed requirements of the given engine and generator drive. Tending to have the lowest number of batteries as possible, the right battery type must be selected. The battery storage and fuel storage are complementary energy sources and the aim of optimization task is finding the optimal three-fold data set, [rotational engine speed, number of battery cells, fuel weight].

System optimization

System optimization approaches

The optimization problem is specified by the function of the total weight of the system that includes in the first approximation only the weight of fuel, engine, generator and batteries. Minimization of the function is performed under the constraints derived from the mathematical model of the system i.e. the maximal weight, the minimum 96 h energy output, the maximal battery discharging current etc. and the natural bounds of system parameters i.e. weight cannot be less than zero, speed of engine must not be out of the allowed range etc. The most of the constraints are nonlinear functions of the system variables therefore finding the minimum of total system weight can be observed as the nonlinear constrained optimization problem.

The general problem description is to minimize the objective function *F(X)* subjected to the set of nonlinear constraint functions *g_i(X)* (9),

$$g_i(X) \leq 0, i = 1 \dots p \tag{9}$$

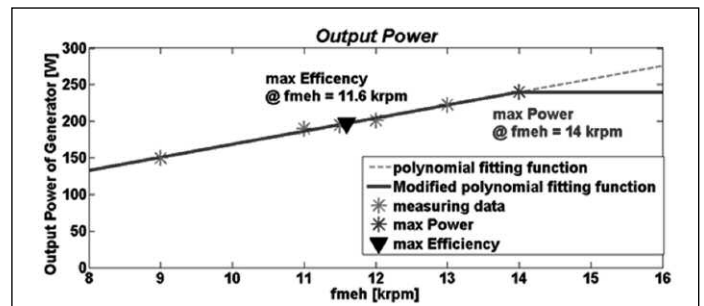


Fig. 4: Measured output DC electrical power for an OS-30 four-stroke engine running with gasoline

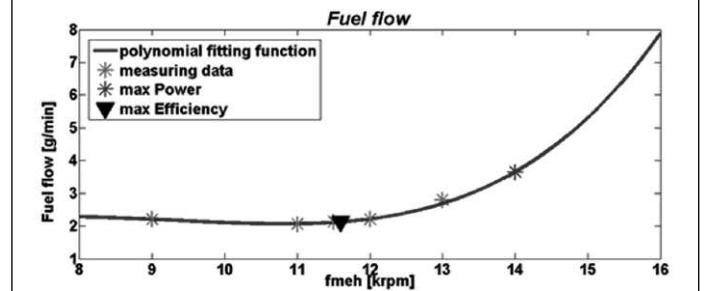


Fig. 5: Fuel mass flow for an OS-30 four-stroke engine running with gasoline

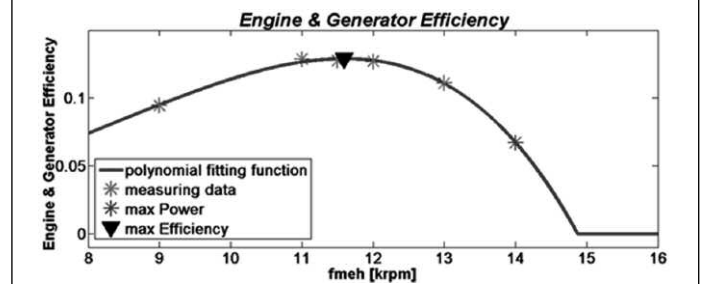


Fig. 6: Engine/generator efficiency for an OS-30 four-stroke engine running with gasoline

For the WPS, the optimization working point (*X*) is defined by three variables: the engine speed, the number of battery cells in parallel (*m*) and the total weight of fuel (*Q_f*). The optimization problem is specified by the function of the total weight of system, *F(X)* (10),

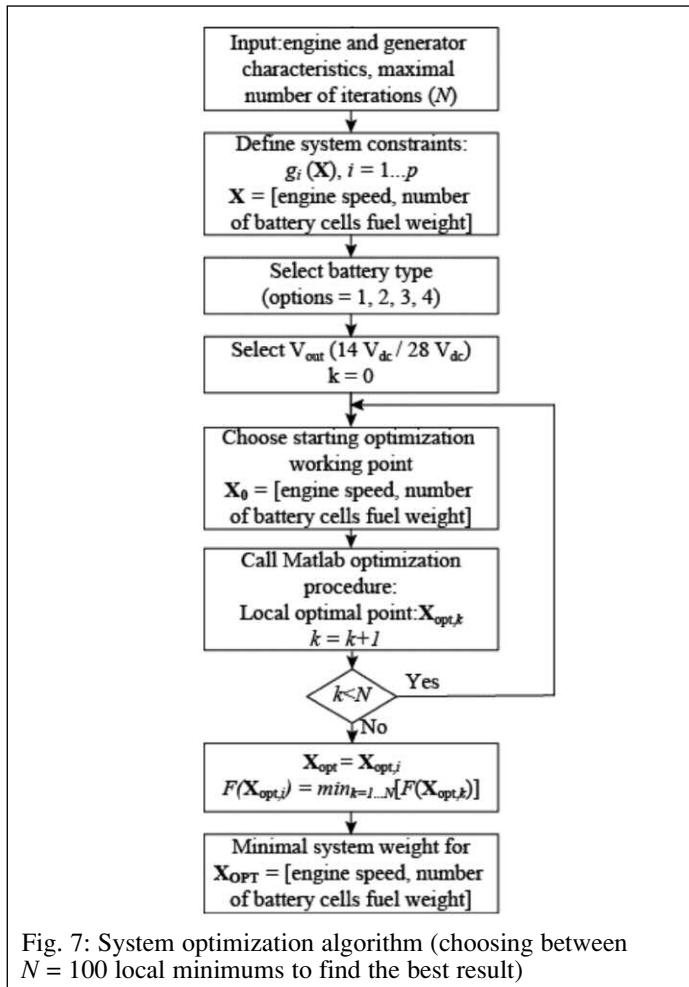
$$F(X) = Q_e + Q_g + Q_f + m \cdot n \cdot Q_b \tag{10}$$

that includes in the first approximation only the weight of fuel (*Q_f*), engine (*Q_e*), generator (*Q_g*), and battery pack (*m · n · Q_b*), where *Q_b* is the weight of a single battery, *m · n* is the number of batteries in the battery pack) (10).

In the literature, constrained optimization problems are solved either by direct methods or by using unconstrained optimization. For the purpose of comparison and checking the correctness of results, two programs, one based on Sequential Unconstrained Minimization Techniques (SUMT) [30] and another based on direct method, Sequential Quadratic Programming (SQP) [31] are implemented with MATLAB. The system optimization algorithm is presented as the flowchart in Fig. 7.

System optimization results

The optimization procedures were run for both possibilities of output voltage, 14 *V_{dc}* and 28 *V_{dc}* and for four different battery types (see Table 2 and Fig. 7):



- Type 1: Li-Ion ANR26650 (70 g per cell);
- Type 2: VARTA Li-Polymer batteries (17 g per cell);
- Type 3: VARTA Li-Polymer batteries (24 g per cell);
- Type 4: KOKAM Li-Polymer battery type (115 g per cell).

The battery data sheets can be found in [23], [24], and [25]. None of these battery types satisfies all desired features: small weight, high maximal charging current and high nominal voltage. Regarding the minimum system weight, the optimization procedures returned Type 4 as the best choice and Type 1 as the worst choice. This shows that the battery type with the highest gravimetric energy (VARTA) is not the optimal solution.

Comparing to the other battery types, battery Type 4 is suitable since the maximal charging current is higher than the current delivered by engine/generator, which allows the minimal number of batteries to be connected in parallel, i.e. the optimal battery pack consists of 7 battery units connected in series. The optimization results shows that for $14 V_{dc}$ and $28 V_{dc}$ output voltage, the same system weight can be achieved. $28 V_{dc}$ is selected as it results in lower currents and lower electrical losses.

Simulation results

For the optimal system design parameter set, a simulation is performed to check if the optimized system behaves well under a specified 96 hours Load Profile. That means that an optimization method has returned the design three-fold set [engine speed, number of cells in parallel, fuel weight] such that there is enough fuel and enough battery storage to provide the needed power for the specific 96 h Mission Profile. The final results of the optimization for the wearable power system with the OS FS-30 Surpass engine

are summarized in Table 3. Table 3 includes also the following results: the engine working operating point, the total fuel consumption, the intervals of charging periods and the remaining fuel. The calculated total needed mass of fuel is shown to be more than enough for 4 days Mission Profile (remaining fuel = 95 g). The simulation proved that such a system can accomplish both the required power demands and the weight requirement as the total system weight is estimated to be 2.8 kg and there is enough additional weight (1.2 kg) for the auxiliary system components.

The simulation results presented in Fig. 8 shows the Load Profile (black line), the battery state of charge (SOC, dark gray line) and the engine on/off state signal (light gray top line) over the operating time of 96 h. When the engine is on, the state signal is at low level, the battery state of charge, SOC (dark gray line) increases. When the state signal is at high level, the engine is off, SOC follows the Load Profile (black line) meaning that if output power is low around 3 W the battery discharges slowly and for the high peaks of output power, the battery discharge is very fast. The battery is discharged to 20 % of its capacity and charged at a constant current to 80 % capacity after which the engine is shut down and the charging ceases. It is assumed that the battery is initially 100 % fully charged. The result of the simulated 96 h operation is that there is still sufficient energy left in the battery after the testing time.

To prove the starting assumption that the system requirements cannot be met by running the engine with the methanol fuel mixture with lower energy density of 20 MJ/kg, the tests were repeated for the same engine-generator system using the methanol/oil mixture. The engine characteristics were interpolated in the similar manner as it was presented for the gasoline case. The fitting defined the maximal engine-generator efficiency to be 15.5 % at 13386 rpm rotor speed. The performed simulation for 96 h mission has returned the total weight of 3.89 kg including auxiliary system components. This result confirms the starting assumption that the weight constraint of 4 kg cannot be satisfied using methanol.

DC-DC optimization results

As the optimized system provides $28 V_{dc}$ output and the system needs a second voltage output of $14 V_{dc}$, a buck converter (DC-DC converter) is added to the WPS between the battery and the load

Table 3: The optimization results for gasoline and battery

System Weight (excluding auxiliary systems)	2857 g
Fuel Consumption	1309 g
Total Fuel Weight	1404 g
Remaining Fuel	95 g
Engine Operating Point	
Engine Speed	12358 rpm
Mass Fuel Flow	2.34 g/min
Engine and Generator Efficiency	12.4 %
Battery Information	
Battery Type	Type 4
Output Voltage	28 VDC
Power at Battery Input	200 W
Number of Cells in series (n)	7
Number of Parallel battery Strings (m)	1
Battery Charging Information	
Number of Charging Periods	16
Maximal Duration of Charging	54 min
Minimal Duration of Charging	23 min

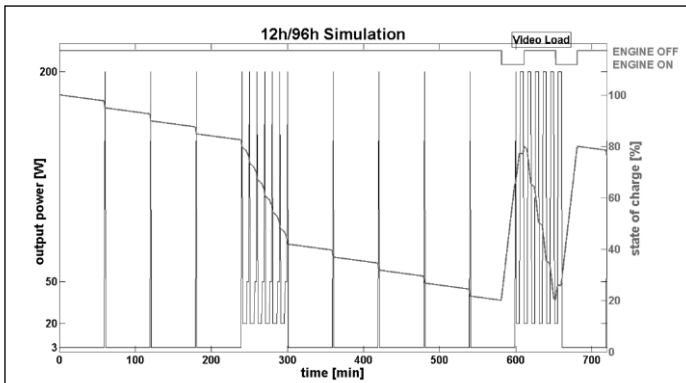


Fig. 8: Simulation results for the case of 28 V_{dc} output and KOKAM battery type: output power (Mission Profile) and battery state of charge in %: 96 hours operating time (zoomed first 12h).

Table 4: Output power levels and time periods

Duration	Power Level
1121 min	3 W
169 min	20 W
57 min	50 W
93 min	200 W

output. The buck converter was selected since it is a simple and robust topology, and due to the limited implementation time in the competition it allows fast construction and testing. Other DC-DC converter topologies may have a higher efficiency, such as resonant converters, however these were not investigated in this study. The parameters of the buck converter do not depend on the parameters of the IC engine/generator/battery system so the buck converters optimization can be performed independently from the optimization presented in the previous section. On the other side, selecting the optimal converter structure i.e. number of buck converters operating in parallel and their weight optimizations are two interleaved processes. Namely, the optimization of the buck-converter is investigated in [32], while the complete system is considered in this paper.

At first, with the assumption that a 20 W and a 200 W buck converter (switching frequency of 250 kHz) could satisfy the output power demand, two buck converter prototypes were designed and then optimized regarding weight, cf. Fig. 14. Subsequently, their efficiency curves were measured, cf. Fig. 13, and used as the starting point for the optimization of the number of parallel converters what is presented in the following subsection.

Number of converters

The load has a wide range of output power levels and applied time intervals (Table 4 derived from Table 1). The lowest 3 W load is applied for the longest time. Therefore, the considered DC-DC converter system is obligated to have a high efficiency for light loads since the lost energy must be provided by the gasoline and results in a higher system weight.

The DC-DC converter efficiency drops at the light load due to losses such as capacitive switching losses, gate drive or control losses, which do not decrease (linearly) with output power. A possibility to increase the efficiency at light load is to connect together converter systems with lower and higher nominal power ratings in parallel and to operate different converter combinations for each load level, so that the operating point of the converter that is mainly providing the output power is near its nominal value [33]. Usually, the parallel converters are designed in a way that they all have the same nominal power, i.e. at full load the power is

equally provided by all converters. In the case of a complicated load profile consisting of different power levels, a system design with parallel converters with different nominal powers providing the output power in different time intervals could result in the better system efficiency compared to the design of equal converter units.

In the WPS mission profile, for relatively long periods a low power is required. Accordingly, parallel-connected DC-DC converters with different nominal powers are taken into consideration. Since it is important not only to consider the efficiency but also the time interval of operation, finding the optimal number of parallel DC-DC converters, their nominal power levels and operating points can be solved as a problem of minimization of total energy losses [34].

The efficiency of a converter is defined by:

$$\eta_n = P_{out,v}/P_{in,v} \tag{11}$$

where $P_{out,v}$ is the output and $P_{in,v}$ the input power of the considered (v -th) converter. The losses of the converter can be calculated by means of efficiency and the output power

$$P_{L,v} = P_{in,v} - P_{out,v} = \frac{1 - \eta_v}{\eta_v} P_{out,v} \tag{12}$$

so that the energy wasted during the mission profile $E_{L,v}$, i.e. converted in heat, is defined by

$$E_{L,v} = \int_0^T \frac{1 - \eta_v}{\eta_v} P_{out,v} dt \tag{13}$$

where T is the duration of the mission profile. In the simplest case, the efficiency of a single converter is optimized, so that the waste energy is minimal. The degrees of freedom could be, for example, adapting control modes/current shapes [35] or optimising passive components for special operation conditions. With several parallel converters optimized for different power levels, the output power sharing is not needed and the losses of the converters system depend on individual DC-DC converters characteristics and also on how the output power is distributed between the units. Consequently, the optimization of the converters nominal power levels $P_{nom,v}$ and the converter operating points δ_v is performed in order to minimize the total losses. The quality criteria i.e. the objective function F to be minimized is given by

$$F = \sum_{j=1}^{N_{level}} \sum_{i=1}^{N_{conv}} P_L(\delta_{ij}, P_{nom,i}) \tag{14}$$

where N_{level} is the number of power levels inside of the mission profile, N_{conv} is the number of parallel-connected converters, δ_{ij} is the operating point of i -th converter at j -th output power level, $P_{nom,i}$ is the nominal power of i -th converter and P_L is the function of power losses. The values of the losses are based on experimental measurements, for a 200 W and a 20 W system, and on analytical models for interpolating the loss functions. Table 5 presents the numerical values for the losses as well as the average efficiency, the nominal power distribution and the additional fuel weight due to converters losses.

It can be seen that more than 30 % of the original system losses can be saved by optimizing the nominal power levels and the operating points. Thus, a system with two parallel connected converters is the most optimal. Increasing the parallel converter number results in a distribution where the optimization algorithm sets one nominal power to zero, i.e. returns two systems.

Number of converters	1	2	3
Total energy loss	460 kW _s	317.2 kW _s	317.2 kW _s
Additional fuel due to converter losses	76.76 g	52.87 g	52.87 g
Efficiency	93.6 %	95.5 %	95.5 %
Optimal power levels	200 W	3 /197 W	0 /3 /197 W

A similar result can be obtained by the following consideration: let us assume that a converter, A, has an efficiency of η_A for an output load power level P_{out} , where this power level is less than converter A's nominal power of 200 W. Therefore converter A is operating with a reduced efficiency, i.e. a non-optimal operating point. If we replaced the converter A with a converter B, which is optimized for the power level P_{out} and has an efficiency of η_B , the fuel savings at P_{out} would be Δm ,

$$\Delta m = \frac{P_{out} \cdot \Delta t}{LHW \cdot \eta_{eg} \cdot \eta_c} \left(\frac{1}{\eta_A} - \frac{1}{\eta_B} \right) \quad (15)$$

where LHW is the heating value of the fuel (43 MJ/kg for gasoline), $\eta_{eg} \cdot \eta_c$ is the efficiency of the engine, generator and the inverter (approximately 13.5 %) and Δt is the total operating time of converter B and P_{out} is the output power. To estimate the real benefits of the new converter B, the additional PCB and inductor weight of the new converter as well as the decreased reliability should not be neglected. If the additional PCB approximately weights 10 g and an inductor weight is 10 g, then it would be necessary to have the fuel weight savings of more than 20 g in order to obtain a total weight reduction. Applying (15) the minimum efficiency of the additional converter to save at least 30 g of fuel can be calculated for the load demands $P_{out} = 3$ W and $P_{out} = 50$ W. Due to the load characteristics, the total energy processed by 20 W and 3 W loads is the same hence the minimum efficiency for the 20 W converter is the same as for the 3 W converter. In Fig. 9, the results of this analysis are plotted.

The efficiency, η_B , is represented for two different values of the fuel savings, 20 g and 30 g, and the plot clearly shows the fact that it is necessary to use more efficient converter for the higher fuel savings. Another important conclusion is that a single 200 W converter, such that its efficiency at 50 W is higher than 80 %, and at 3 W and 20 W higher than 85 %, would be the best solution for the system, when the savings of 30 g of fuel is necessary.

In Fig. 10, the efficiency of the additional 3 W converter $\eta_B = \eta_B(\eta_A, \eta_{EG})$ as the function of the first converter efficiency and the efficiency of engine/generator is presented. For increasing engine efficiency a higher efficiency of the second converter is needed in order to save 30 g of the total weight. This gives stronger reasons to use only one converter.

Optimal weight of converters

The converter weights have to be optimized as the total system weight has to be less than 4 kg. Higher switching frequency results in a smaller inductor size, however the losses within the system will rise as well as the amount of the additional fuel. Accordingly, the optimal frequency for which the sum of the inductor weight and the weight of the additional fuel is minimal has to be determined. In order to solve this problem, a special algorithm has been implemented. The total additional weight, i.e. the weight of the used inductor plus the weight of additional fuel is estimated based on the switching losses, and inductor geometry and losses. The input data for the algorithm are the converter output voltage of $14 V_{dc}$, the power levels, and the databases for available magnetic cores and MOSFETs. According to the algorithm, a

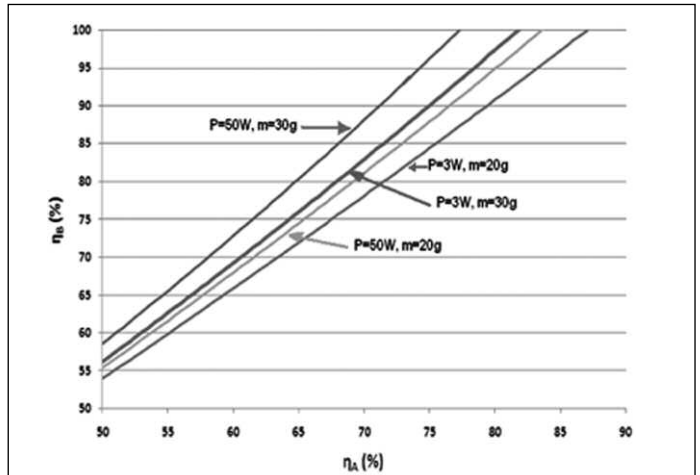


Fig. 9: Minimum efficiency of additional 3 W and 50 W converters in order to save 10 g and 30 g of fuel

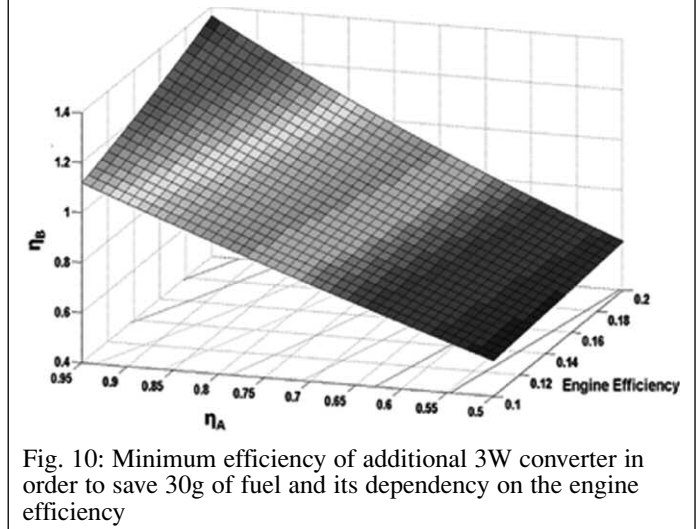


Fig. 10: Minimum efficiency of additional 3W converter in order to save 30g of fuel and its dependency on the engine efficiency

switching frequency is searched and the best core is identified in order to optimize the total additional weight. The results are the core type and dimensions, the number of turns needed to obtain certain inductance, the system efficiency and the optimal switching frequency.

In order to estimate MOSFET power losses, a simple switching model is used [36, 37]. The optimal switching frequency is not expected to be high therefore more complicated models that include parasitic inductances [38] have not been used. The MOSFET losses are decoupled into several loss mechanisms and calculated using the MOSFET datasheets. The following loss mechanisms have been distinguished: gate drive losses (due to effective gate capacitance), losses due to the parasitic output capacitance, losses due to MOSFET on-resistance, and losses due to the reverse recovery current. The losses inside the control chip have been taken into account as well, because the control chip is supplied by the converter's input voltage.

To estimate the power losses in the selected inductor, the losses due to DC resistance, skin effect and non-linearity of the core (hysteresis characteristics of the core) have been considered. The DC resistance is calculated simply using the information about the length of the copper wire that is needed for the inductor and the area of its cross section. The AC resistance is estimated by [39]:

$$R_{AC} \approx L_{r0}/(\pi\delta D) \tag{16}$$

where L is the total length of the used wire, ρ_0 is copper’s resistivity, D is wire’s diameter and δ is skin depth. The inductor current can be represented as an infinite sum of harmonics, and for each of these harmonics a different AC resistance has to be used. Since the first switching frequency harmonic is the most dominant, the losses due to the skin effect were estimated using the effective value of the current’s first harmonic and using the AC resistance calculated at the switching frequency. The losses due to the hysteresis characteristic of the used core are a function of the geometry and material properties and have been estimated using the Steinmetz equation [40],

$$P = V \cdot C \cdot f^\alpha \cdot B^\beta \tag{17}$$

where V is the volume of the selected core, f is the converter switching frequency, B is the amplitude of the excursion of magnetic inductance in the inductors core, and the parameters C , α and β are constants that depend on the core’s material.

All the power losses caused by inserting the DC-DC converter into the system must be compensated by the energy produced by the engine and/or by the additional fuel. The additional fuel is estimated using the information about the engine’s efficiency and the fuel heating value. In this way, the total additional weight (the weight of fuel, copper wire and the used core) is expressed as a function of the switching frequency so that the implemented algorithm searches for the switching frequency that provides the minimal additional weight. The optimization algorithm is presented in Fig. 11.

Fig. 12 presents the result of the analysis in the case of a 200 W converter. The cores are taken from the Magnetics powder core database [39]. According to Fig. 12, from 50 kHz to 150 kHz the additional weight falls because the inductor weight influence is more significant than the influence of the additional fuel needed to compensate the converter’s losses. As the frequency increases, the converter losses rise and the fuel weight has more influence than the inductor’s weight. It can be seen that the optimal frequency is near 150 kHz. The steps in the curve are a consequence of the discrete weight values of the analyzed inductors.

In Table 6, some possible solutions that could be used for the converter’s inductor with its corresponding switching frequency are summarized.

Results

In order to provide data for the converter number optimization, and verify the implemented algorithm, two prototypes were constructed. The first is a 20 W 28 V/14 V and the second is a 200 W 28 V/14 V buck converter both using a switching frequency of 250 kHz. The 20 W converter is implemented with LM25576 step-down switching regulator [41] and the 200 W converter as a synchronous buck converter with LM5116 buck controller [40] and SUD50N06-16P MOSFETs [42]. These components were selected in order to build an optimal converter with high reliability and low losses. The implemented 200 W converter is presented in Fig. 13. The efficiency measurements results and their comparison with the theoretical loss model are shown in Fig. 14.

Regarding the system efficiency and the earlier analysis about the minimal converter efficiency, it is concluded that a single converter

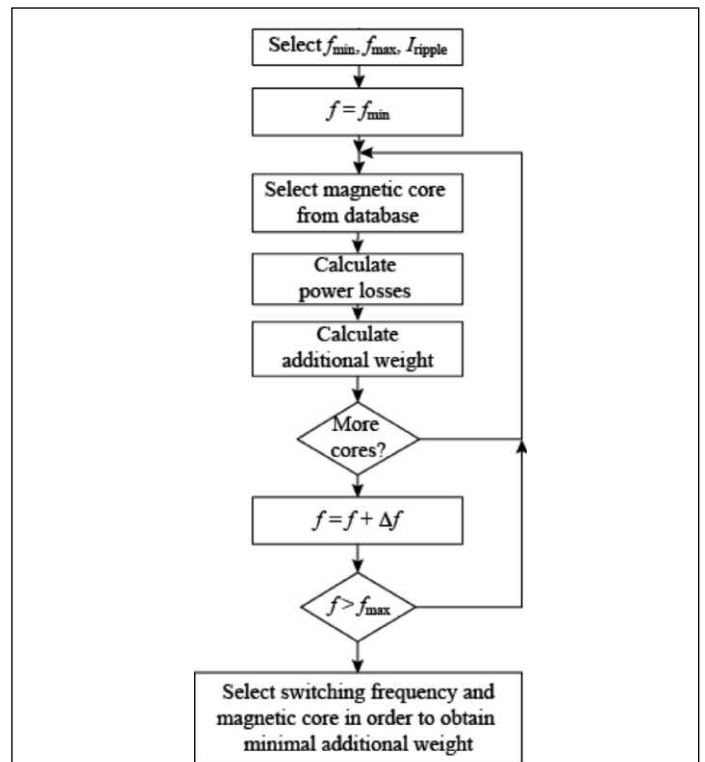


Fig. 11: The optimization algorithm for minimizing the additional weight introduced by dc-dc converter ($f_{min} = 50$ kHz, $f_{max} = 500$ kHz)

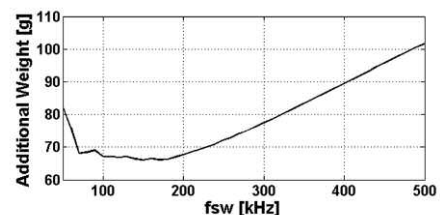


Fig. 12: Additional weight of 200 W converter for different switching frequencies

f_{sw} (kHz)	Material type	Type of core	Number of turns
50	MPP200	55307	30
100	HF60	58848	27
150	HF160	58118	19

is an optimal solution. The measurements performed with prototypes that have integrated power components (in the case of LM25576) or, single chip solution for the control stage with additional power components (in the case of LM5116 and SUD50N06-16P) have shown that these prototypes would fulfil the requirements regarding the minimal efficiency of the converter at different power loads even when a non optimized switching frequency is applied. It should be emphasized that these solutions are not unique, and that other components could be selected as well.

The inductor core selection from the set of available cores is based on the implemented algorithm for determining the minimal additional weight. The main purpose of the measurements in the case of 20 W converter is to provide necessary data for the analysis presented in previous section. As it can be seen from Fig. 14, the effi-

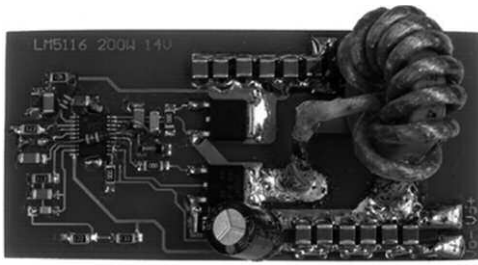


Fig. 13: Photograph of implemented 200 W converter (dimensions 7.5 cm x 3.5 cm, weight = 33 g).

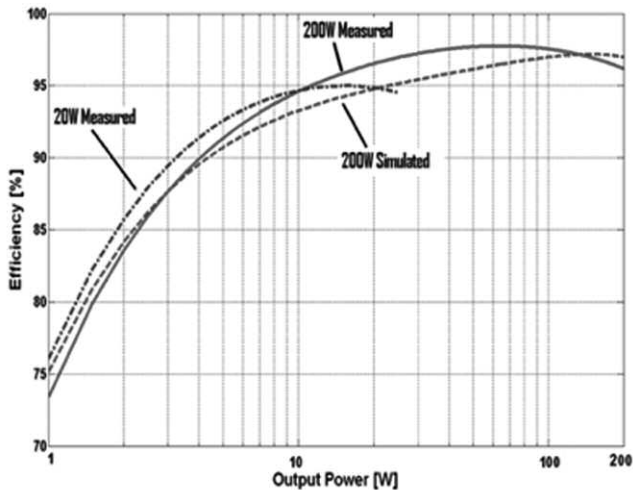


Fig. 14 : Efficiency of 20 W and 200 W converters ($f_{sw} = 250$ kHz).

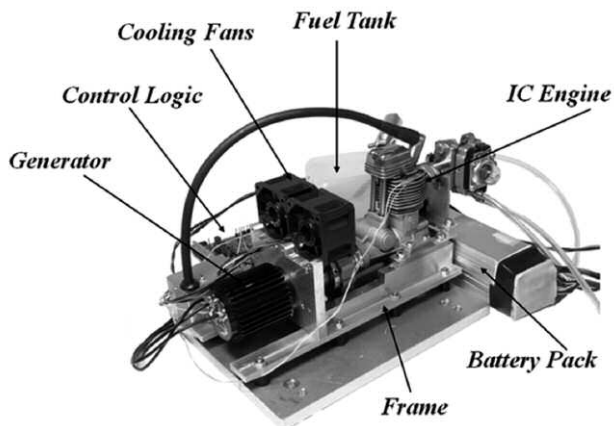


Fig. 15: The individual parts of the realized prototype of WPS with total competition weight of 3989.6g (the system housing is not shown)

ciency based on the applied loss model follows the measured efficiency adequately and it is confirmed that the model is accurate enough to estimate the additional fuel weight and the optimal switching frequency range. Based on the results, a 200 W converter with the efficiencies of approximately, 87 % for 3 W load, 96 % for 20 W load and 97 % for 50 W load, could be the solution although 250 kHz is not the optimal switching frequency. The implemented 200 W converter fulfils the conditions that were set in the starting analysis concerning the number of converters and the desired efficiency of the buck converter. Having an additional converter in the system would provide a small benefit from the point of view of a total system weight.

Table 7: Final WPS weight estimate

System Components	Weight
Engine + Generator	0.4 kg + 0.3 kg
Fuel	1.5 kg
Battery Pack	0.8 kg
Power and Control Electronics	0.4 kg
Mounting Hardware and Frame	0.5 kg
Total	3.9 kg

Finally, the inductor is realized using HF160 and the core size 58206 [40]. The selected switching frequency is 140 kHz as the best results according to the measurements were achieved at this frequency which at the same time belongs to the optimal frequency range between 100 kHz and 200 kHz. The measured efficiency of the optimized 200 W converter at the switching frequency of 140 kHz is: 87 %, 96.4 %, 97 %, and 96.2 % respectively for 3 W, 20 W, 50 W and 200 W output power levels. The average efficiency of the converter is 95.1 % for the specified load profile.

Final optimization results

According to the system optimization presented in the first part and the optimization of 28/14 V buck converter, a prototype of the wearable power system has been constructed, cf. Fig. 15. The overall system weight estimate of the proposed WPS is summarized in Table 7.

Conclusions

The paper gives the starting point on how to design an optimal power system for a specified mission profile under weight and power constraints. The proposed WPS comprises lithium-based rechargeable batteries, an OS FS-30 Surpass engine, a three-phase permanent magnetic brushless DC motor with power electronics elements, i.e. AC-DC inverters and DC-DC converters. The optimization of the overall system is presented as problem of finding the minimum of a function subjected to nonlinear constraints. The optimal design results returned by Matlab optimization and simulation procedures are: an output voltage of $28 V_{dc}$, seven KOKAM Li-Polymer batteries in series, the optimal engine operating point around the point of maximal efficiency and the gasoline/oil mixture as fuel. In the second part of the paper, the concentration is directed to the output power electronics part, i.e. DC-DC buck converters implemented between the load and the battery pack to provide the output voltage level of $14 V_{dc}$. The optimal number of converters is determined according to the correlation between the minimum efficiency of the additional converter and the weight savings that could be obtained by the converter. Based on the analysis and the load profile, it is shown that the selection of only one 200 W converter is the optimal solution for the system. To keep the total weight of the WPS as low as it is possible, the optimal switching frequency of the buck converter is found to be in the range between 100 kHz to 200 kHz. Several core materials and core types are employed for the buck inductor. In order to verify the loss models, two experimental converters have been constructed and tested. By measuring their efficiency, it is proved that a simple converter is the optimal solution. Finally, the first prototype is constructed based on the optimization presented in this paper. The total system weight including fuel and housing is less than the required 4 kg. The proposed methodology can be applied to high power systems.

References

[1] [Online] <http://www.dod.mil/ddre/prize/topic.html>: Wearable power prize rules, 2008.

[2] [Online] <http://www.dod.mil/ddre/prize/topic.html>: Wearable power prize load profile for bench test, 2008.

[3] I. Kovacevic, S. D. Round, J. W. Kolar, and K. Boulouchos: Optimization of a wearable power system, in Proc. of 11th IEEE Workshop on Control and Modeling for Power Electronics (COMPEL), Zurich, Switzerland, August 18 – 20, 2008, pp. 1-6.

[4] C. Shu and B. Jeyasurya: Power system transfer capability studies using constrained optimization technique, in Proc. of IEEE Power Engineering Society General Meeting, Canada, July 13-17, 2003, pp. 882-889.

[5] M. Zahran, A. Dmowski, B. Kras, P. Biczal, and J. Drazkiewicz: PV battery wind-turbine public-grid hybrid power supply for telecom.-equipment, system management and control, in Proc. of 35th Intersociety Energy Conversion Engineering Conf. and Exhibit, Las Vegas, USA, July 24-28, 2000, pp. 1252-1260.

[6] B. Ali Baharuddin, S. Kamaruzzaman, M. Abd. Rahman, M. Y. Othman, A. Zaharim, and A. M. Razali: Hybrid photovoltaic diesel system in a cable car resort facility, European J. of Scientific Research, vol. 26, no. 1, pp. 13-19, January 2009.

[7] D. Houy, J. Steinshneider, and T. Davies: Fuel cell / Li-ion battery hybrid power system for the advanced space suit, in Proc. of 3rd International Energy Conversion Engineering Conf., San Francisco, California, August 15-18, 2005, AIAA 2005-5677.

[8] B. Huang, Xi Shi, and Y. Xu: Parameter optimization of power control strategy for series hybrid electric vehicle, in Proc. of IEEE Congress on Evolutionary Computation, Vancouver, Canada, July 16-21, 2006, pp. 1989-1994.

[9] P. Thounthong: Control of fuel cell/battery hybrid source for electric vehicle applications, ECTI Trans. Electrical Eng., Electronics, and Communications, vol. 5, no. 2, August 2007.

[10] S. Lu, D. H. Meegahawatte, S. Guo, S. Hillmansen, C. Roberts, and C.J. Goodman: Analysis of energy storage devices in hybrid railway vehicles, in Proc. of ICRE Conf., China, March 25-28, 2008, pp 1-6.

[11] T. Ogawa, H. Yoshihara, S. Wakao, K. Kondo, and M. Kondo: Energy consumption analysis of FC-EDLC hybrid railway vehicle by dynamic programming, in Proc. of European Conf. Power Electronics and Applications, Denmark, September 2-5, 2007, pp. 1-8.

[12] National Academy of Sciences, (Washington D.C., 2002), Combat hybrid power system component technologies: technical challenges and research priorities (ch.6) [Online]: (http://www.nap.edu/openbook.php?record_id=10595).

[13] E. Holliday and D. E. Keiter: Control electronics for palm power 35W free-piston stirling engine, in Proc. of Int. Energy Conversion Engineering Conf., San Francisco, California, August 15-18, 2005, Paper 97.

[14] S. Fish and T.B. Savoie: Simulation-based optimal sizing of hybrid electric vehicle components for specific combat missions, IEEE Transactions on Magnetics, vol. 37, no. 1, pp. 485-488, January 2001.

[15] W. Schmitt: Modeling and simulation of photovoltaic hybrid energy systems-optimization of sizing and control, in Proc. of 29th IEEE Photovoltaic Specialists Conf., New Orleans, May 19-24, 2002, pp. 1656-1659.

[16] J. Ab. Razak, K. Sopian, Y. Ali, M. A. Alghoul, A. Zaharim, and I. Ahmad: Optimization of PV-wind-hydro-diesel hybrid system by minimizing excess capacity, European J. of Scientific Research, vol. 25, no. 4, pp. 663-671, January 2009.

[17] A. Abbasi, and J. Zhenhua: Design and analysis of a fuel cell/gas turbine hybrid power system, in Proc. of IEEE Power and Energy Society General Meeting - Conversion and Delivery of Electrical Energy in the 21st Century, Pittsburgh, PA, USA, July 20-24, 2008, pp. 1-6.

[18] S. B. Sprague, Sang-Won Park, D. C. Walther, A. P. Pisano, and A. C. Fernandez-Pello: Development and characterization of small-scale rotary engines, International J. of Alternative Propulsion, vol. 1, no. 2/3, pp. 275 – 293, 2007.

[19] [Online] <http://www.quallion.com>, August 2008.

[20] D. Dunn-Rankin, E. Martins Leal, and D. C. Walther: Personal power systems, Progress in Energy and Combustion Science, vol. 31, no. 5-6, pp. 422-465, 2005

[21] OS Engines Japan, [Online] <http://www.osengines.com/>

[22] ATE GmbH, [Online] <http://www.ate-system.de/en/our-range/rotors.html>.

[23] A123Systems Battery Datasheet, [Online] <http://www.a123systems.com> .

[24] VARTA Battery Datasheet, [Online] <http://www.varta-microbattery.com>.

[25] KOKAM Battery Datasheet, [Online] http://www.kokam.com/english/product/battery_main.html.

[26] F. R. Kalhammer, B. M. Kopf, D. H. Swan, V. P. Roan, and M. P. Walsh: Status and prospects for zero emissions vehicle technology, Report of the ARB Independent Expert Panel, April 13th, 2007.

[27] V. Pop, H. J. Bergveld, P. H. L. Notten, and P. L. Regtien: State-of-the-art of battery state-of-charge determination, Measurement Science and Technology, vol. 16, no. 12, pp. 93-110, December 2005.

[28] F. Hoffart: Extending Li-Ion battery life, Power Systems Design Europe - Special Report, pp. 25, April 2008.

[29] S. Wiak, M. Dems and K. Kom'za: Maximum wind power control using torque characteristics in a wind diesel system with battery storage, in Recent Developments of Electrical Drives, Springer Netherlands, 2006, pp. 385-396.

[30] G. N. Vanderplaats: Numerical optimization techniques for engineering design, New York: McGraw Hill, 1984.

[31] P. T. Boggs and J. W. Tolle: Sequential quadratic programming, Acta Numerica Cambridge University Press, pp.1-000, 1996.

[32] M. Vasic, S. D. Round, J. Biela, J. W. Kolar: Mission profile based optimization of a synchronous-buck DC-DC converter for a Wearable Power System, in Proc. of 6th IEEE International Power Electronics and Motion Control Conf. (IPEMC), Wuhan, China, May 17-20, 2009, pp. 1384 -1389.

[33] B. Eckardt and M. Maerz: A 100kW automotive power train dc-dc converter with 25kW/dm3 by using SiC, in Proc. of International Conf. Power Electronics (PCIM), Nuernberg, Germany, May-Jun, 2006. pp. 185-190.

[34] J. Biela, S. Waffler, and J. W. Kolar: Mission profile optimized modularization of hybrid vehicle DC-DC converter system, in Proc. of 6th IEEE International Power Electronics and Motion Control Conference, Wuhan, China, May 17-20, 2009, pp. 1390-1396.

[35] S. Waffler and J.W. Kolar: A novel low-loss modulation strategy for high-power bi-directional buck-boost converters, in Proc. of the ICPE 2008, Daegu, South Korea, October 22-26, 2008, pp. 889-894.

[36] J. Klein,: Synchronous buck MOSFET loss calculations with Excel model, Fairchild Semiconductor Application Notes AN6005, January 2006.

[37] International Rectifier Datasheet: Power MOSFET selection for non-isolated dc-dc converters, International Rectifier, 2003.

[38] W. Eberle, Z. Zhang, Yan-Fei Liu, and P. C. Sen: A simple analytical switching loss model for buck voltage regulators, in Proc. of 23rd IEEE Annual Conf. Of Applied Power Electronics, Jun 15-19, 2008, pp. 3780 – 3786.

- [39] R. Erickson, D. Maksimovic, *Fundamentals of power electronics* (2nd edition), Kluwer 2000.
- [40] Core Design Manual and Catalog, Magnetics Inc, [Online] <http://www.mag-inc.com/>
- [41] National Semiconductors Buck Regulators Datasheet, National Semiconductors Santa Clara, Calif. [Online] <http://www.national.com/>
- [42] Vishay MOSFET Datasheet, Vishay Intertechnology, Inc., [Online] <http://www.vishay.com>

The authors



Ivana F. Kovačević (SM'10) graduated from the University of Belgrade, Serbia, Faculty of Electrical Engineering, Department for Electronics, in 2006 (with honors). In June 2007 she joined the Power Electronic Systems Laboratory at the Swiss Federal Institute of Technology (ETH), Zurich, Switzerland as a postgraduate student. She received the M.Sc. degree in electrical engineering and information technology and Ph.D. degree from ETH Zurich in 2008 and 2012, respectively, focusing on lifetime modeling of power modules and 3D electromagnetic modeling of Electromagnetic Interference (EMI) Filters. She is currently working as a Postdoctoral Assistant in the Power Electronic Systems Laboratory at ETH Zurich. Her research activities are focused on multi-domain modeling and optimization of power electronics systems and components.



Simon Round received the B.E. (Hons) and Ph.D. degrees from the University of Canterbury, Christchurch, New Zealand, in 1989 and 1993, respectively. From 1992 to 1995 he held positions of Research Associate in the Department of Electrical Engineering at the University of Minnesota and Research Fellow at the Norwegian Institute of Technology, Trondheim, Norway. From 1995 to 2003 he was a Lecturer/Senior Lecturer in the Department of Electrical and Electronic Engineering at the University of Canterbury where he performed research on power quality compensators, electric vehicle electronics, and cryogenic power electronics. From 2004 to 2008 he was a Senior Researcher in the Power Electronic Systems Laboratory at ETH Zurich, Switzerland where he researched in the areas of ultra-compact power converters, applications of silicon carbide power devices, and three-phase ac-ac converters. In October 2008, he joined ABB Switzerland as the Control Platform Technology Manager for the Power Electronics and Medium Voltage Drives Business Unit. He is currently the Head of Platform Management at the ABB Power Conversion Business Unit.



Miroslav Vasić was born in Serbia 1981. He received the M.S. degree from the University of Belgrade, School of Electrical Engineering, Serbia, in 2005. He got a master and PhD degree in Industrial Electronics from the University of Madrid, Spain, in 2008 and 2010, respectively. Since 2010 he has been working as a researcher in Centro de Electronica Industrial (CEI), Madrid. His research interests include switching mode power supplies, RF circuit design and digital control applied to power electronics.



Johann W. Kolar (F'10) received his M.Sc. and Ph.D. degree (summa cum laude / promotio sub auspiciis praesidentis rei publicae) from the University of Technology Vienna, Austria. Since 1982 he has been working as an independent international consultant in close collaboration with the University of Technology Vienna, in the fields of power electronics, industrial electronics and high performance drives. He has proposed numerous novel converter topologies and modulation/control concepts, e.g., the VIENNA Rectifier, the SWISS Rectifier, and the three-

phase AC-AC Sparse Matrix Converter. Dr. Kolar has published over 400 scientific papers at main international conferences and over 150 papers in international journals and has filed more than 110 patents. He was appointed Professor and Head of the Power Electronic Systems Laboratory at the Swiss Federal Institute of Technology (ETH) Zurich on Feb. 1, 2001. The focus of his current research is on AC-AC and AC-DC converter topologies with low effects on the mains, e.g. for data centers, More-Electric-Aircraft and distributed renewable energy systems, and on Solid-State Transformers for Smart Microgrid Systems. Further main research areas are the realization of ultra-compact and ultra-efficient converter modules employing latest power semiconductor technology (SiC and GaN), micro power electronics and/or Power Supplies on Chip, multi-domain/scale modeling/simulation and multi-objective optimization, physical model-based lifetime prediction, pulsed power, and ultra-high speed and bearingless motors. He has been appointed an IEEE Distinguished Lecturer by the IEEE Power Electronics Society in 2011. He received 7 IEEE Transactions Prize Paper Awards and 7 IEEE Conference Prize Paper Awards. Furthermore, he received the ETH Zurich Golden Owl Award 2011 for Excellence in Teaching and an Erskine Fellowship from the University of Canterbury, New Zealand, in 2003. He initiated and/or is the founder/co-founder of 4 spin-off companies targeting ultra-high speed drives, multi-domain/level simulation, ultra-compact/efficient converter systems and pulsed power/electronic energy processing. In 2006, the European Power Supplies Manufacturers Association (EPSMA) awarded the Power Electronics Systems Laboratory of ETH Zurich as the leading academic research institution in Power Electronics in Europe. Dr. Kolar is a Fellow of the IEEE and a Member of the IEEJ and of International Steering Committees and Technical Program Committees of numerous international conferences in the field (e.g. Director of the Power Quality Branch of the International Conference on Power Conversion and Intelligent Motion). He is the founding Chairman of the IEEE PELS Austria and Switzerland Chapter and Chairman of the Education Chapter of the EPE Association. From 1997 through 2000 he has been serving as an Associate Editor of the IEEE Transactions on Industrial Electronics and since 2001 as an Associate Editor of the IEEE Transactions on Power Electronics. Since 2002 he also is an Associate Editor of the Journal of Power Electronics of the Korean Institute of Power Electronics and a member of the Editorial Advisory Board of the IEEJ Transactions on Electrical and Electronic Engineering.